Electric-field effects on electronic tunneling transport in magnetic barrier structures

Yong Guo, Hao Wang, and Bing-Lin Gu
Department of Physics, Tsinghua University, Beijing 100084, People's Republic of China

Yoshiyuki Kawazoe
Institute for Materials Research, Tohoku University, Sendai 980-8577, Japan

(Received 16 February 1999; revised manuscript received 15 July 1999)

Electronic transport properties in magnetic barrier structures under the influence of an electric field have been investigated. The results indicate that the characteristics of transmission resonance are determined not only by the structure and the incident wave vector but also strongly by the electric field. It is shown that the transmission coefficient at resonance in the low-energy range is suppressed by applying the electric field for electron tunneling through the magnetic barrier structure, arranged with identical magnetic barriers and wells. It is also shown that the transmission resonance is first enhanced up to optimal resonance, and then suppressed with further increased electric field for electron tunneling through the magnetic barrier structure, arranged with unidentical building blocks. Strong suppression of the current density is also found in the magnetic barrier structure, arranged with two different building blocks.

Electronic transport phenomenon in the magnetic modulated two-dimensional electron gas (2DEG) has attracted tremendous interest.[1–10] Experimentally, recent technological advances allowed one to create lateral superlattices based on a spatially periodic magnetic modulation, which is of nonpotential type and gives rise to peculiar behavior of the charge carriers.[4] Theoretically, Matulis, Peeters, and Vasilopoulos[5] found the quantum transport through magnetic barrier (MB) structures possesses wave-vector filtering properties. Guo *et al.*[7] investigated tunneling properties through simple MB structures with different magnetic barriers and periodic and quasiperiodic MB superlattices. Moreover, the magnetic minibands in the energy spectrum are formed.[8] Classical transport properties in a MB superlattice under the influence of time-dependent (ac) electric fields have been explored.[9] Studies on quantum transport in finite MB superlattices created by depositing ferromagnetic stripes on top of a heterostructure indicate that an external electric field strengthens the anisotropy of the transmission.[10]

In this paper we study tunneling properties in different types of MB structures under applied biases. The noticeable wave-vector-dependent and electric-field-dependent tunneling features are revealed.

We consider a 2DEG system [in the (x,y) plane] subject to a perpendicular magnetic field (along z direction). The magnetic field is taken to be homogeneous along the y axis and varies along the x axis. A MB quantum structure can be obtained by arranging two different blocks A and B, each of which consists of one magnetic barrier [with height B_i and width d_i $(i=1,2)$] and one magnetic well [with depth $-B_i$ and width d_i $(i=1,2)$]. The Schrödinger equation is written in the framework of the effective-mass approximation under the influence of an external electric field as

$$\left(\frac{1}{2m^*}[\mathbf{P}+e\mathbf{A}_i]^2-eFx\right)\Psi(x,y)=E\Psi(x,y), \qquad (1)$$

where m^* is the effective mass of electron, F is the external electric field along the x direction, e is the proton's charge, and $\mathbf{A}_i=(0, A_i(x),0)$ is the Landau vector potential. We express all quantities in dimensionless units by using the cyclotron frequency $\omega_c=eB_0/m^*$ and the magnetic length $l_B=\sqrt{\hbar/eB_0}$. For GaAs and an estimated $B_0=0.1$ T we have $l_B=813$ Å, $\hbar\omega_c=0.17$ meV;[5] m^* can be taken as $0.067m_e$ (m_e is the free-electron mass). The wave function can be written as a product, $\Psi(x,y)=e^{ik_y y}\Phi(x)$, where k_y is the wave vector in the y direction. Accordingly, we obtain the following one-dimensional Schrödinger equation

$$\left(\frac{d^2}{d^2x}-[A_i(x)+k_y]^2+\frac{2eV_a x}{L_x}+2E\right)\Phi(x)=0. \qquad (2)$$

The function $V(x,k_y,V_a)=[A_i(x)+k_y]^2/2-eV_a x/L_x$ can be interpreted as an effective electric potential. $V_a=FL_x$ is the applied bias, and $L_x=2d_1+2d_2$ is the length along the x direction. In the left and right regions, the wave functions are free-electron wave functions, which can be written as $\Psi_l(x,y)=e^{ik_y y}(e^{ik_l x}+re^{-ik_l x})$, and $\Psi_r(x,y)=\tau e^{ik_y y}e^{ik_r x}$, where $k_l=\sqrt{2E-[A_l(x)+k_y]^2}$, $k_r=\sqrt{2(E+eV_a)-[A_r(x)+k_y]^2}$, and r and τ are reflection and transmission amplitudes, respectively, which can be obtained by matching the wave functions and their derivatives at the edges of magnetic barriers and magnetic wells.

In magnetic barrier and well regions, Eq. (2) can be solved analytically, and the wave function $\Psi_i(x,y)$ can be written as a combination of two linearly independent confluent hypergeometric functions[11] $U(\frac{1}{4}\lambda_i, \frac{1}{2}, \xi_i^2)$ and $M(\frac{1}{4}\lambda_i, \frac{1}{2}, \xi_i^2)$,

$$\Psi_i(x,y)=\exp(ik_y y)\exp(-\tfrac{1}{2}\xi_i^2)[C_i U(\tfrac{1}{4}\lambda_i, \tfrac{1}{2}, \xi_i^2) + D_i M(\tfrac{1}{4}\lambda_i, \tfrac{1}{2}, \xi_i^2)], \qquad (3)$$

where C_i and D_i are constants to be determined from the boundary conditions, $\xi_i=\sqrt{m^*\omega_i/\hbar}(x-x_i^0)$, $\omega_i=eB_i/m^*$,

$$x_i^0(x)=\begin{cases} -\dfrac{\hbar k_y}{eB_1}+\dfrac{m^*V_a}{eB_1^2L_x}, & 0\leqslant x<d_1 \\ 2d_1+\dfrac{\hbar k_y}{eB_1}+\dfrac{m^*V_a}{eB_1^2L_x}, & d_1\leqslant x<2d_1 \\ 2d_1-\dfrac{\hbar k_y}{eB_2}+\dfrac{m^*V_a}{eB_2^2L_x}, & 2d_1\leqslant x<2d_1+d_2 \\ 2d_1+2d_2+\dfrac{\hbar k_y}{eB_2}+\dfrac{m^*V_a}{eB_2^2L_x}, & 2d_1+d_2\leqslant x<2d_1+2d_2 \end{cases} \tag{4}$$

and

$$\lambda_i=\begin{cases} 1-\dfrac{2}{\hbar\omega_1}\left(E+\dfrac{m^*F^2}{2B_1^2}-\dfrac{\hbar k_yF}{B_1}\right), & 0\leqslant x<d_1 \\ 1-\dfrac{2}{\hbar\omega_1}\left(E+\dfrac{m^*F^2}{2B_1^2}+\dfrac{\hbar k_yF}{B_1}+2ed_1F\right), & d_1\leqslant x<2d_1 \\ 1-\dfrac{2}{\hbar\omega_2}\left(E+\dfrac{m^*F^2}{2B_2^2}-\dfrac{\hbar k_yF}{B_2}+2ed_1F\right), & 2d_1\leqslant x<2d_1+d_2 \\ 1-\dfrac{2}{\hbar\omega_2}\left(E+\dfrac{m^*F^2}{2B_2^2}+\dfrac{\hbar k_yF}{B_2}+2e(d_1+d_2)F\right), & 2d_1+d_2\leqslant x<2d_1+2d_2. \end{cases} \tag{5}$$

The transmission coefficient of electrons through the MB structure is given by

$$T(E,k_y,V_a)=\frac{k_r}{k_l}|\tau|^2. \tag{6}$$

The current density J_x can be derived from the transmission coefficient by the following expression:

$$\begin{aligned} J_x&=\frac{2e}{(2\pi)^2\hbar}\int_{k_x>0}dk_xdk_y[f(E,E_f^l) \\ &\quad -f(E,E_f^r)]T(E,k_y,V_a)\frac{\partial E}{\partial k_x} \\ &=\frac{e\sqrt{m_0^*}}{\sqrt{2}\pi^2\hbar^2}\int_0^\infty dE\ \sqrt{E}[f(E,E_f^l) \\ &\quad -f(E,E_f^r)]\int_{-\pi/2}^{\pi/2}(\cos\theta)T\left(E,\left(\frac{2m_0^*E}{\hbar^2}\right)^{1/2}\sin\theta,V_a\right)d\theta \\ &=J_0\int_0^\infty dE\sqrt{E}[f(E,E_f^l)-f(E,E_f^r)]\int_{-1}^1 T(E,\overline{\theta},V_a)d\overline{\theta}, \end{aligned} \tag{7}$$

where $J_0=e\sqrt{m_0^*}/\sqrt{2}\pi^2\hbar^2$ and $f(E,E_f^l)$ and $f(E,E_f^r)$ are the Fermi-Dirac distribution functions in the left and right electrodes. When $T=0$ K, the above equation becomes

$$J=J_0\int_{E_0}^{E_F}dE\sqrt{E}\int_{-1}^1 T(E,\overline{\theta},V_a)d\overline{\theta}, \tag{8}$$

where $E_0=(E_F-eV_a)\Theta(E_F-eV_a)$ and Θ is the step function.

Figure 1 presents the numerical results for electron tunneling through two MB structures, each of which is an arrangement with two identical building blocks A ($B_1=0.1$ T and $d_1=1$). Here and in the following, eV_a is given in units of $\hbar\omega_c$. In Figs. 1(a1), 1(a2), and 1(a3), we can see that at zero bias, transmission resonance is unity, and for different k_y, transmission resonance occurs at different incident energy. Under an applied bias, the transmission coefficient at resonance is suppressed and the degree of suppression is different for electrons with different k_y. Moreover, resonance peaks shift to lower-energy regions, and some peaks disappear with the increased field. The external electric field strengthens the anisotropy of the transmission coefficient with wave vector k_y. Similar results have been obtained in Figs. 1(b1), 1(b2), and 1(b3), where there is a zero magnetic-field region $l=3$ within barriers. The most obvious discrepancy in this case compared to those exhibited in Figs. 1(a1), 1(a2), and 1(a3) is that the transmission spectrum becomes more complex, and more and sharper peaks appear.

Figure 2 shows numerical results for electron tunneling through a MB structure arranged with two different blocks A and B under positive and negative biases. The direction of the electric field $\mathbf{F}$ and the applied bias V_a are opposite to each other. For positive bias, the direction of the electric field is from right to left. One can easily see that at zero bias, the transmission coefficient at resonance is off unity, and for different k_y, the difference of the suppression of the transmission coefficient at resonance is enlarged, in contrast to the case for electron tunneling through the MB structure arranged with two identical blocks. Here what greatly strikes us is that under the positive bias, the transmission resonance is first enhanced up to optimal resonance and then suppressed by further increasing positive bias. Under the negative bias, there still exists a transition of transmission resonance. However, an optimal transmission resonance occurs at larger amplitudes of the bias. Here we would like to point

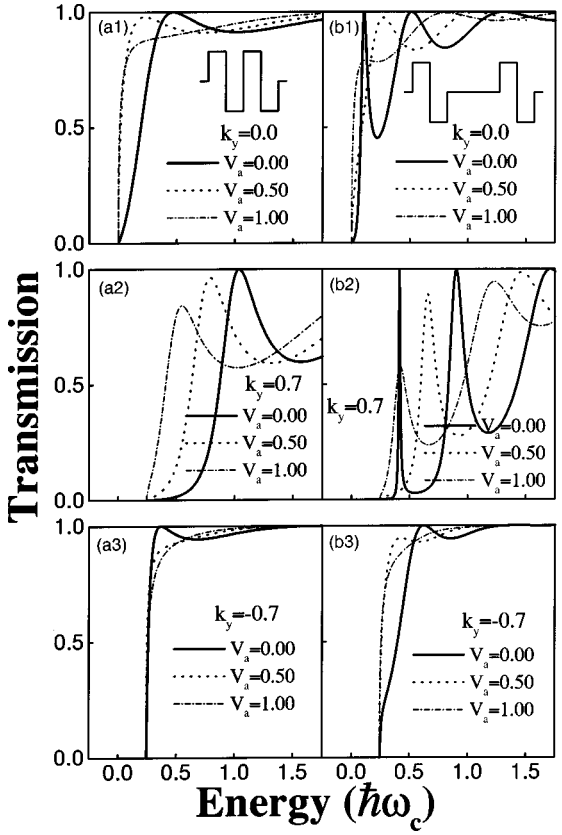

FIG. 1. Transmission through two MB structures, each of which is arranged with two identical blocks A ($B_1=0.1$ T and $d_1=1$), $l=3$.

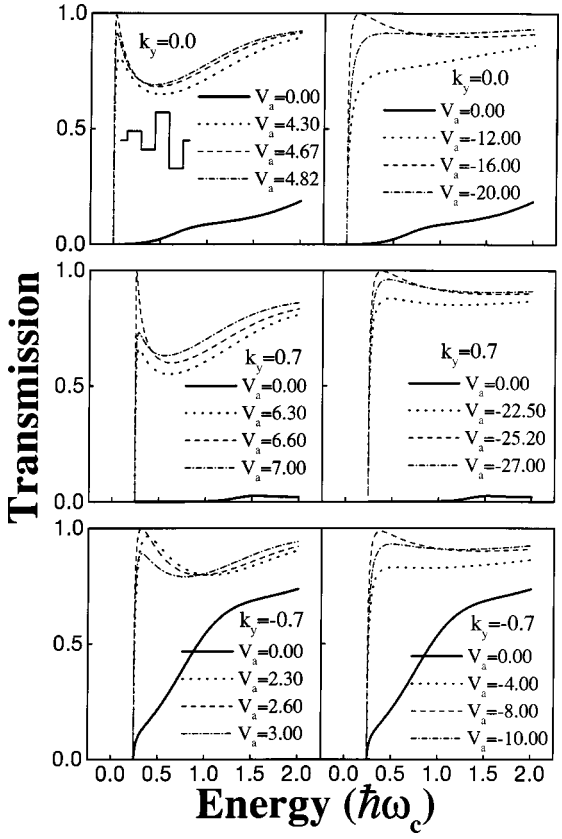

FIG. 2. Transmission through one MB structure, which is an arrangement with block A ($B_1=0.1$ T and $d_1=1$) and block B ($B_2=0.3$ T and $d_2=1$) under applied positive and negative biases.

out that the optimal transmission resonance under a negative bias is for the second peak resonance, while in the positive bias case, optimal resonance is for the first peak. In the former cases, the first peak disappears before it reaches optimal resonance. A similar transition of the transmission resonance can also be found in the case of electron tunneling through another type of MB structure in which two building blocks have different widths and same heights.

Most tunneling properties obtained in the MB structure[5,7] have been successfully explained by using the concept of k_y-dependent effective electric potentials. In this work, the effective electric potential $V(x,k_y,V_a)=[A_i(x)+k_y]^2/2-eV_ax/L_x$ is more complex, which depends not only on the wave vector k_y but also on the bias V_a, so it can be called a k_y-dependent and electric-field-dependent effective potential. Figure 3 shows two model MB structures and their corresponding effective potential, where $q_1=B_1d_1$ and $q_2=B_2d_1$. For electrons with $k_y>0$ transport through a double-MB structure, the corresponding effective potential is an electric double-barrier structure in which transport is the tunneling through the double barriers. For the $k_y<0$ case, the effective electric potential is multiple wells in which the process of electron motion is transport through states above quantum wells.[5] Here we should notice the well-known fact, i.e., the transmission coefficient at resonance is usually unity in a symmetric electric double-barrier structure at zero bias. If an electric field is applied to the symmetric structure, the symmetric feature of the structure cannot be retained and the transmission coefficient at resonance is reduced. For the same reason, the transmission coefficient in the asymmetric

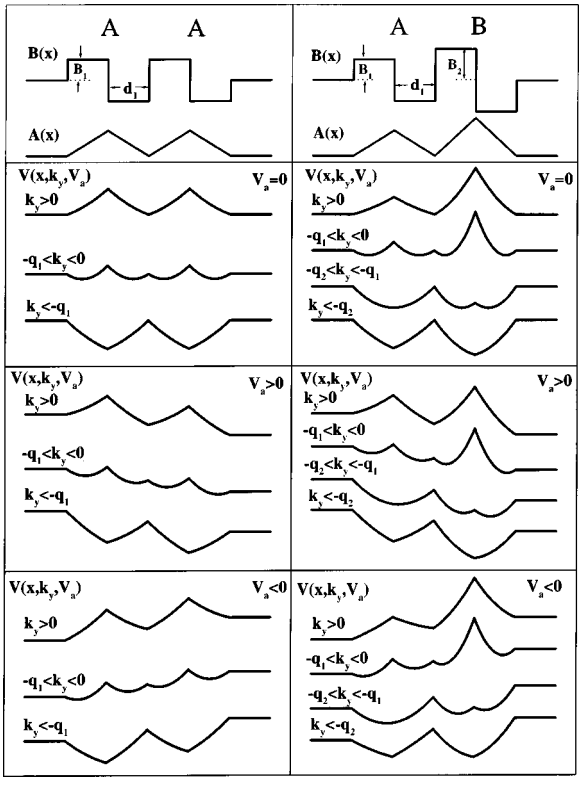

FIG. 3. Two model MB structures and the corresponding effective potentials.

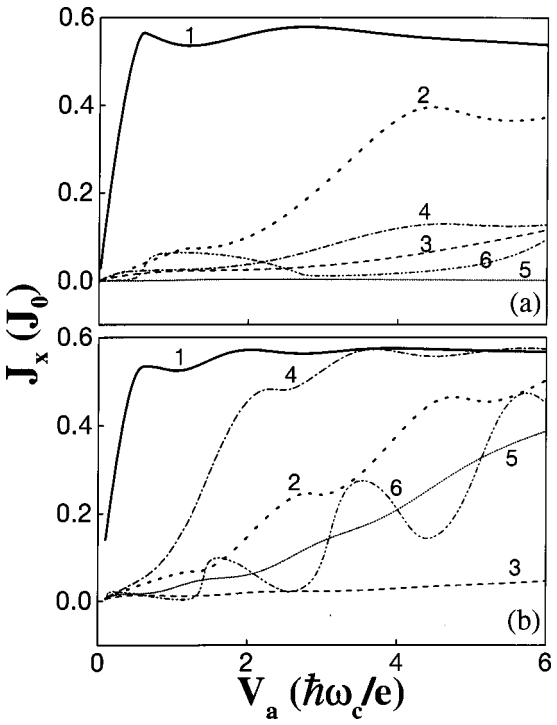

FIG. 4. Current density through eight MB structures.

electric double-barrier structure is small. However, complete tunneling can occur in the asymmetric electric structure if the transmission coefficient for the left barrier is exactly the same as that for right one. Therefore, keeping these facts in mind, we have no difficulty in understanding the transition of transmission resonance found in the MB structure. For electron transport through the MB structure of identical blocks, the potential profile is equivalent to electric barrier or well structures of identical blocks. So in this case at zero bias, we can see complete tunneling as in the electric structures of identical barriers and wells. For electron tunneling through the MB structure of different blocks, the potential profile is equivalent to the electric structures of unidentical barriers or wells, and for different k_y, the corresponding electric structure differs greatly. Under biases, the symmetry of the effective potential has been greatly changed. Therefore, in the transmission spectrum we can see rich k_y-dependent and electric-field-dependent transitions of the transmission resonance.

In Fig. 4 we show the current density J_x for electron tunneling through eight MB structures. The Fermi energy is set to be $E_F=0.6$. In Fig. 4(a), curve 1 is for one MB structure arranged with two identical blocks A ($B_1=0.1\,\mathrm{T}$ and $d_1=1$); curves 2 and 3 are for one MB structure arranged with different blocks A ($B_1=0.1\,\mathrm{T}$ and $d_1=1$) and B ($B_2=0.3\,\mathrm{T}$ and $d_2=1$) under positive and negative biases; curves 4 and 5 are for one MB structure with different blocks A ($B_1=0.1\,\mathrm{T}$ and $d_1=1$) and B ($B_2=0.1\,\mathrm{T}$ and $d_2=2$) under positive and negative biases; curve 6 is for one structure arranged with two blocks A ($B_1=0.1\,\mathrm{T}$ and $d_1=1.95$) and B ($B_2=0.3\,\mathrm{T}$ and $d_2=1$). Here we take amplitude values of the current density and the negative biases in order to draw all calculated results in the same figure. It can be seen that J_x-V_a characteristic exhibits obvious negative-differential conductivity. The current is drastically suppressed for electron tunneling through the MB structure with different blocks. Another noticeable fact is that current density can be enhanced in MB structure with unidentical blocks (see curve 6) if we properly choose the parameters of building blocks. Similar results for the other four MB structures can be found in Fig. 4(b), where the only difference from Fig. 4(a) is that there is a zero magnetic field region $l=3$ within magnetic barriers. The noticeable discrepancy in this case is that the current spectrum becomes more complex and more current peaks appear.

In summary, features of tunneling properties through MB structures depend not only on the structure and the incident wave vector, but also strongly on the applied electric field. For electron tunneling through the MB structure with identical building blocks, the transmission resonance is suppressed in the low-energy range with increased electric field. For electron tunneling through the MB structure with unidentical blocks, the resonance is first enhanced up to optimal resonance and then suppressed with increased electric field. The current density is also strongly suppressed in the latter case.

Three of us (Y. G., H. W., and B.-L. G.) would like to acknowledge that this project was supported in part by the National High Technology Development Program of China (Grant No. 715-010-0011) and by the Research Foundation of Tsinghua University (Grant No. 98jc082).

[1] M. A. McCord and D. D. Awschalom, Appl. Phys. Lett. **57**, 2153 (1990).

[2] M. L. Leadbeater *et al.*, J. Appl. Phys. **69**, 4689 (1991); K. M. Krishnan, Appl. Phys. Lett. **61**, 2365 (1992); W. Von Roy *et al.*, J. Magn. Magn. Mater. **121**, 197 (1993); R. Yagi and Y. Iye, J. Phys. Soc. Jpn. **62**, 1279 (1993).

[3] A. K. Geim, Pis'ma Zh. Eksp. Teor. Fiz. **50**, 359 (1989) [JETP Lett. **50**, 389 (1990)]; S. J. Bending, K. von Klitzing, and K. Ploog, Phys. Rev. Lett. **65**, 1060 (1990).

[4] H. A. Carmona *et al.*, Phys. Rev. Lett. **74**, 3009 (1995); P. D. Ye *et al.*, *ibid.* **74**, 3013 (1995); S. Izawa *et al.*, J. Phys. Soc. Jpn. **64**, 706 (1995).

[5] M. Matulis, F. M. Peeters, and P. Vasilopoulos, Phys. Rev. Lett. **72**, 1518 (1994).

[6] Heung-Sun Sim *et al.*, Phys. Rev. Lett. **80**, 1501 (1998).

[7] Yong Guo *et al.*, Phys. Rev. B **55**, 9314 (1997); J. Appl. Phys. **83**, 4545 (1998); J. Phys.: Condens. Matter **10**, 1549 (1998).

[8] I. S. Ibrahim and F. M. Peeters, Phys. Rev. B **52**, 17 321 (1995); A. Krakovsky, *ibid.* **53**, 8469 (1996).

[9] Oleg M. Yevtushenko and Klaus Richter, Phys. Rev. B **57**, 14 839 (1998).

[10] Y. M. Mu, Y. Fu, and M. Willander, Superlattices Microstruct. **22**, 135 (1997).

[11] H. Cruz, A. Hernández-Cabrera, and P. Aceituno, J. Phys.: Condens. Matter **2**, 8953 (1990); M. Abramowitz and I. A. Stegun, *Handbook of Mathematical Functions* (Dover, New York, 1968), p. 504.